AIAA JOURNAL
Vol. 40, No. 8, August 2002

Jet–Cavity Interaction Tones

Ganesh Raman*
Illinois Institute of Technology, Chicago, Illinois 60616
and
Edmane Envia† and Timothy J. Bencic‡
NASA John H. Glenn Research Center at Lewis Field, Cleveland, Ohio 44135

A fundamental study of resonant tones produced by jet–cavity interaction over a wide range of flow conditions covering both subsonic and supersonic speeds is described. Two significant findings emerge. For the jet–cavity configurations investigated, a suitably defined reduced frequency parameter allows for a global classification of all jet–cavity tones into two main types. For the first type, the reduced frequency depends on the jet Mach number, whereas for the second type, the reduced frequency is independent of the jet Mach number. We propose simple correlations for the frequency of both types of tones. Based on earlier research, we had expected that the traditional classifications of cavity flows into the open, transitional, or closed variety would be insensitive to small changes in Mach number and would depend primarily on the cavity's *L/D* ratio. However, use of the novel high-resolution photoluminescent pressure sensitive paint shows that these classifications are actually quite sensitive to the jet Mach number for jet–cavity interactions. However, these classifications provide no guidance for determining tone type, amplitude, or frequency.

I. Introduction

FLOWS over cavities occur in aircraft weapons bays, wheel wells, in-flight refueling ports, pressure vents in the space shuttle's cargo bay, and in a host of other situations. Flows over cavities exhibit significant changes in the steady and unsteady near-field pressure that are critical in both aeronautical and space applications. Edge, cavity, and screech tones are all ostensibly produced by very similar phenomena. These tones are generally attributed to embryonic disturbances in the shear layer that grow while convecting downstream and whose interaction with an edge, or shock-cell, produces impulsive pressures that propagate upstream to close a resonant loop. Screech tones and jet–edge interactions have been studied by Powell,[1,2] Crighton,[3] and Howe,[4] among others. A review of advances in understanding screech was provided by Raman.[5] Despite the global similarity between edge, cavity, and screech tones, there are intricate differences that make a universal frequency or amplitude model elusive. The need to study such fine differences between subclasses of flow tones also motivated this work. Our focus is on the interaction of subsonic and supersonic shock-containing jets with a cavity where both screech and cavity tones are theoretically permissible. Note that our experiments are for a jet interacting with a cavity, which is quite different from a cavity in an infinite flight stream.[6–9] However, it is important for us to present our results in the context of existing cavity resonance models, especially because we wish to contribute to the design of cavity resonance suppression techniques. A brief review of the pertinent literature is given hereafter.

The importance of the cavity problem to the aerospace sciences is evident from the vast number of papers written on this subject, starting with the original work of Helmholtz in 1868 (Ref. 10). Models for resonant frequencies produced by flows over cavities were proposed by Rossiter,[6,7] East,[8] Bilanin and Covert,[9] Block,[11] Tam,[12] and Tam and Block.[13] Heller et al.[14,15] and Heller and Bliss[16] made very significant contributions to our understanding of cavity resonance (and methods for its suppression) by providing a vivid description of physical mechanisms occurring during flow–cavity interaction. For further details, the interested reader is referred to review papers by Rockwell and Naudascher,[17] Komerath et al.,[18] Chokani,[19] Shaw,[20] and Lucas et al.[21] In the interest of brevity, the preceding research is not discussed in great detail. However, for our purposes it is important to recognize Rockwell and Naudascher's[17] classification of cavity oscillations into three types: fluid dynamic, fluid resonant, and fluid elastic. In the first type, the cavity oscillations are driven solely by the instability of the shear layer, whereas in the second type, cavity oscillations result from the coupling of the inherent instability of the shear layer with one or more of the cavity's resonant acoustic modes. The third type of oscillation occurs only when the cavity has compliant walls. Our flow situation is fluid resonant, where further subclassifications exist. When flow over the cavity is supersonic, Stallings and Wilcox[22] and Plentovich et al.[23] classified the cavity flows to be open, transitional, or closed. When the shear layer spans the cavity opening, the cavity is considered open, and when the shear layer attaches to the cavity floor, the cavity is considered closed. Intermediate stages are considered transitional.

More recently, the focus has shifted to active control of flows over cavities[24,25] because of the potential for these techniques to suppress resonance over a range of operating conditions for various cavity geometries. However, there is very limited information on the details of subsonic and supersonic shock-containing flows over cavities and associated unsteady pressures in the near field. This current work studies in detail the near-field pressures (both steady and unsteady) during jet–cavity interaction resonance. This paper presents experimental results aimed at understanding physical mechanisms responsible for large pressure amplitudes produced by flow-induced resonance in cavities. Although the jet–cavity interaction problem was initially chosen due to facility limitations, the intriguing results led to a very detailed study.

Our objectives are as follows. Tones produced by jet–cavity interaction are, in some cases, quite different from those produced either by shock-containing jets or by cavities in flight. Many details of the jet–cavity interaction problem remain to be understood. Our overall objective is to go beyond familiar polemics and raise fundamental questions about such complex resonant flows. The differences between jet–cavity interaction and a cavity in a flight stream are important to understand because we intend to eventually use

Presented as Paper 99-0604 at the AIAA 37th Aerospace Sciences Conference, Reno, NV, 11–14 January 1999; received 29 May 1999; revision received 5 February 2002; accepted for publication 18 February 2002.

*Associate Chairman, Aerospace Engineering, Mechanical, Materials, and Aerospace Engineering Department, Associate Professor. Associate Fellow AIAA.
†Aerospace Engineer, Acoustics Branch. Senior Member AIAA.
‡Aerospace Engineer, Optical Instrumentation Technology Branch.

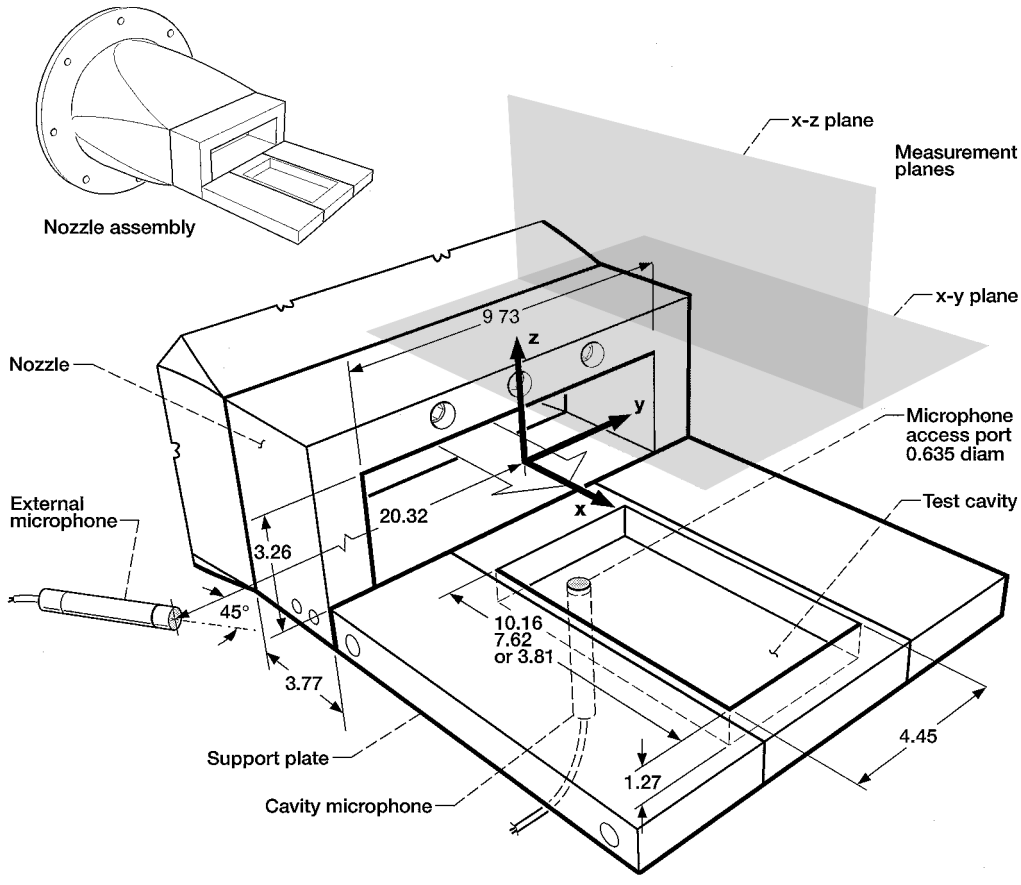

Fig. 1 Jet–cavity configuration, microphones, and measurement planes.

the jet–cavity configuration as a test bed for evaluating active and passive flow resonance control concepts. In addition, one may not always encounter pure Rossiter modes in weapons bays of complex shapes and/or when the weapon is released. Specific objectives for the two related parts of this paper are as follows: 1) We seek to classify all jet–cavity tones into two types. The first type consists of tones produced by shear layer instabilities enhanced by acoustic feedback, and the second type of tones is solely determined by the natural resonance characteristics of the cavity. Tam and Block[13] showed that the latter type of tones are produced at very low Mach numbers. We show that such tones can be produced at Mach numbers between 0.4 and 1.32 when jets interact with cavities of high L/D (6 and above). 2) Our second objective is to reexamine the Stallings and Wilcox[22] classification of flows over cavities (open, transitional, or closed) and its relationship to the frequency and amplitude of the tones. We show that these classifications are very sensitive to Mach number and provide no guidance whatsoever about tone frequency and amplitude. 3) Our third and final objective is to provide benchmark data for those attempting to simulate complex jet–cavity configurations.

The paper is organized as follows: In Sec. II we describe the jet–cavity arrangement and other experimental apparatus. Section III.A discusses results from spark-schlieren flow visualization and correlations between microphones placed internal and external to the cavity. Section III.B covers tones produced by jet–cavity interaction, and Sec. III.C provides a basis to reconcile the nondimensionalized frequencies of these tones. Finally, Sec. III.D discusses the three types of supersonic cavity flows and documents photoluminescent pressure sensitive paint (PSP) results over a range of Mach numbers.

II. Experimental Details

A. Supersonic Flow Facility

Experiments were conducted in a supersonic jet facility at the NASA John H. Glenn Research Center. An existing jet nozzle was modified by adding an adapter to which we could attach rectangular cavities of various dimensions. The cavity dimensions were D (depth) = 1.27 cm and W (width) = 4.445 cm, and L (length) varied as 3.81, 7.62, and 10.16 cm to yield L/D ratios of 3, 6, and 8. The jet flow from a nozzle of exit dimensions 3.26×9.73 cm simulated the flight stream over the cavity. For a more detailed study, we chose two cavities having $L/D = 3$ and 8. Figure 1 shows the nozzle–cavity arrangement. Also shown in Fig. 1 are the location of the internal (cavity) and external microphones and the xy and xz measurement planes in the acoustic near field. The nozzle assembly included a circular-to-rectangular transition piece and a straight section. The contraction area ratio was 4.2, and the length of the nozzle and straight section upstream of the cavity was 18.96 cm.

B. Measurement Techniques

A spark-schlieren system was used for flow visualization. The system included a Palflash light source, a microscope objective, two spherical mirrors (15.24-cm diam, 91.44-cm focal length), and a vertical knife edge. The light source consisted of an electric arc in an inert atmosphere of argon gas that could produce a 1-μs pulse of high intensity light (4 J). Photographs were taken by allowing light from the knife edge to fall directly on Polaroid film. The acoustic measurements were made using 0.635-cm- ($\frac{1}{4}$-in.-) diam B&K microphones. The microphone locations and measurement planes in the near field are shown in Fig. 1. The microphones were calibrated using a B&K pistonphone calibrator, with corrections for day-to-day changes in atmospheric pressure. The sound pressure levels reported in this paper are in decibels (relative to 20 μPa).

C. Photoluminescent PSP

PSP was used to map the steady pressures within the cavity for various operating conditions. The principle of operation for these paints is well documented in the literature[26–28] and will only be mentioned briefly here. Certain chemical compounds, when illuminated by light in a certain band of wavelengths, exhibit luminescence. The luminescent light intensity is inversely proportional to the partial pressure of oxygen. The PSP used in our research was obtained from McDonnell Douglas Aerospace/The Boeing Co. (MDA PF2B). We primed the cavity with a glossy white base coat

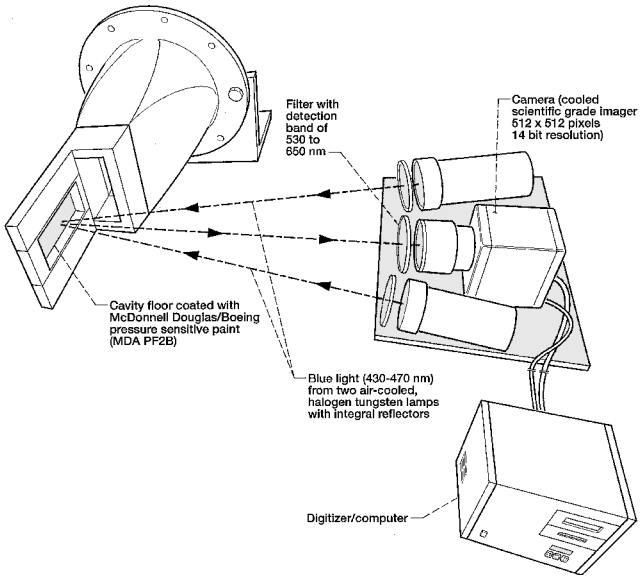

Fig. 2 Photoluminescent PSP apparatus.

(MDA WAL-2) before applying the PSP. The NASA John H. Glenn Research Center PSP system was described by Bencic[29,30] and will only be briefly discussed here. Figure 2 depicts the imaging setup used in the current set of experiments. Two filtered, 75-W tungsten halogen lamps with integral reflectors placed in an air-cooled housing were used to excite the paint molecules. The light wavelength required for excitation (430–470-nm bandwidths) was obtained by selective bandpass filtering of the illumination lamps. Interference filters were used to pass light in the excitation band and reflect unwanted light outside this band. The low-power light sources rendered the photolytic decomposition of PSP insignificant. The camera used in these experiments was a cooled scientific grade imager capable of 14-bit resolution or approximately 16,000 intensity graduations. It had a spatial resolution of 512×512 pixels. The camera was optically filtered to allow only the luminescent light to be incident on the imager (detection bandpass was from 530 to 650 nm). The acquired images were processed using an intensity-based data reduction technique. This technique requires the two images, a wind-off, I_{ref}, reference image, and a wind-on, I_{data}, data image to determine the magnitude of the pressure measurements. By taking the ratio of I_{ref} and I_{data}, we corrected nonuniformities in paint application and lighting. An a priori, or batch, PSP calibration that depended on the composition of the paint was applied to the ratio image, and an in-situ calibration using data from static pressure taps and thermocouples (for temperature correction) on the cavity floor corrected the initial calibration.

D. Minimization of PSP Errors Using a Temperature Correction

When documenting pressure patterns on the cavity floor using PSP, one has to consider temperature variations caused by the jet flow on the cavity floor. Oglesby et al.[31] have emphasized the importance of correcting PSP for temperature sensitivity, which is caused by at least three factors: 1) the luminescence process, 2) the solubility of oxygen in the paint matrix (especially when the luminophore is dissolved in a silicone polymer matrix), and 3) the quenching reaction. The correction was accomplished by first applying temperature-sensitive paint (TSP) to map the temperature on the cavity floor. The calibration for TSP included both a priori and in situ (using thermocouples on the cavity floor) methods. A temperature correction image was then generated using the expression $T_{\text{cor}} = 1 - \alpha \Delta T$, where $\alpha = 0.0047$ and ΔT is the change in temperature from the wind-off images. Note that the constant α was determined by the paint manufacturer (McDonnell Douglas Aerospace/The Boeing Co.) for the paint used in this work. The PSP measurements were then corrected point-by-point by multiplying the PSP ratio intensity ($I_{\text{ref}}/I_{\text{data}}$) by I_{cor}. The maximum error in the PSP measurements was reduced from 5 to 2% by the temperature correction. For details, the interested reader is referred to Refs. 29 and 30.

III. Results and Discussion

A. General Aspects of Jet–Cavity Interaction

Figure 3 shows spark-schlieren photographs for the jet without the cavity and for cavities with $L/D = 3$, 6, and 8 at a fully expanded jet Mach number $M_j = 1.1$. At this Mach number, the jet without a cavity (Fig. 3a) exhibits a weak antisymmetric oscillation downstream but no screech tones. However, strong tones were measured for all of the cavity cases. The outer shear layer lets us visualize vortical events (shear layer instabilities) when the jet is excited by the jet–cavity interaction tone. Events occurring in the upper shear layer of the jet qualitatively correspond to those in the lower (albeit constrained) shear layer. For example, in Fig. 3b, highly energetic vortices are seen in the upper shear layer near the downstream end of the cavity, and a later case displays the emission of an impulsive feedback shock (Fig. 3d).

Figure 4a shows spectra measured internal and external to the cavity. A microphone flush mounted on the cavity floor ($x/D = 0.7$, $y/D = 0$) documented unsteady pressure levels occurring during cavity resonance. A second microphone outside the flow simultaneously recorded external signals in the near acoustic field (see Fig. 1 for microphone locations). For the spectral analysis, the fast Fourier transform block size was 800 (50×16), and the resulting frequency resolution was 32 Hz for the frequency range from 0 to 25,000 Hz. For most measurements, 100 ensembles produced convergent results. A Hanning window was used with maximum overlap. From the internal and external microphone measurements, two observations can be made. First, the frequencies measured internal and external to the cavity are the same. Second, the amplitudes are about 30 dB higher inside the cavity.

Figure 4b provides sample cross correlations for the two cavities at two Mach numbers. The data in Fig. 4 are for the $L/D = 3$ cavity at $M_j = 1.19$. Note the presence of two tones: a high cross-spectrum magnitude and a sharply peaked coherence. In contrast, for an $L/D = 8$ cavity at $M_j = 0.6$, the coherence is high not only at the tone frequency, but over the entire range from 0 to 3 kHz. This indicates the presence of broadband components of cavity noise that are correlated to the radiated noise.

B. Tones Produced by Jet–Cavity Interaction

Figures 5 and 6 show the frequency and amplitude, respectively, of various tones that occur when jets interact with cavities having $L/D = 3$ and 8. Note the presence of discrete frequency modes or stages of resonance (labelled I–III, in the order of increasing frequency). The suffixes A or B refer to parts of the same mode that are created when a mode disappears and reappears at a higher Mach number. On careful examination of the data of Umeda and Ishii[32] for jet–cavity interactions, it is apparent that the frequency jumps that we obtained were present in their data, too. However, they did not highlight this point. It is encouraging that the frequency jumps could be reproduced in two independent and vastly different experimental facilities. Thus, the possibility of the results being facility dependent is highly improbable. Note from Fig. 5a that as M_j is increased to about 0.47, the $L/D = 3$ cavity supports oscillations in mode III, and only later do modes IA and IIA appear. At supersonic Mach numbers, the cavity produces oscillations in mode IIB before mode IB appears. In comparison, for the $L/D = 8$ cavity (Fig. 5b), at subsonic Mach numbers, as the jet velocity is increased, mode IIA appears first, followed by modes I and IIIA. Furthermore, as the Mach number is increased into the supersonic range, mode I persists, followed by IIIB and IIB. We note that in previous studies on cavities Gharib and Roshko[33] observed a similar absence of the primary mode for some freestream velocities.

Also note that the staging behavior seen in Fig. 5 is similar to that observed in screeching circular jets. In the absence of the cavity, the jet from a convergent nozzle produces tones only when there are shocks, that is, in the underexpanded regime. The frequency of this flow resonance (screech) ranged from 7616 Hz at $M_j = 1.1$

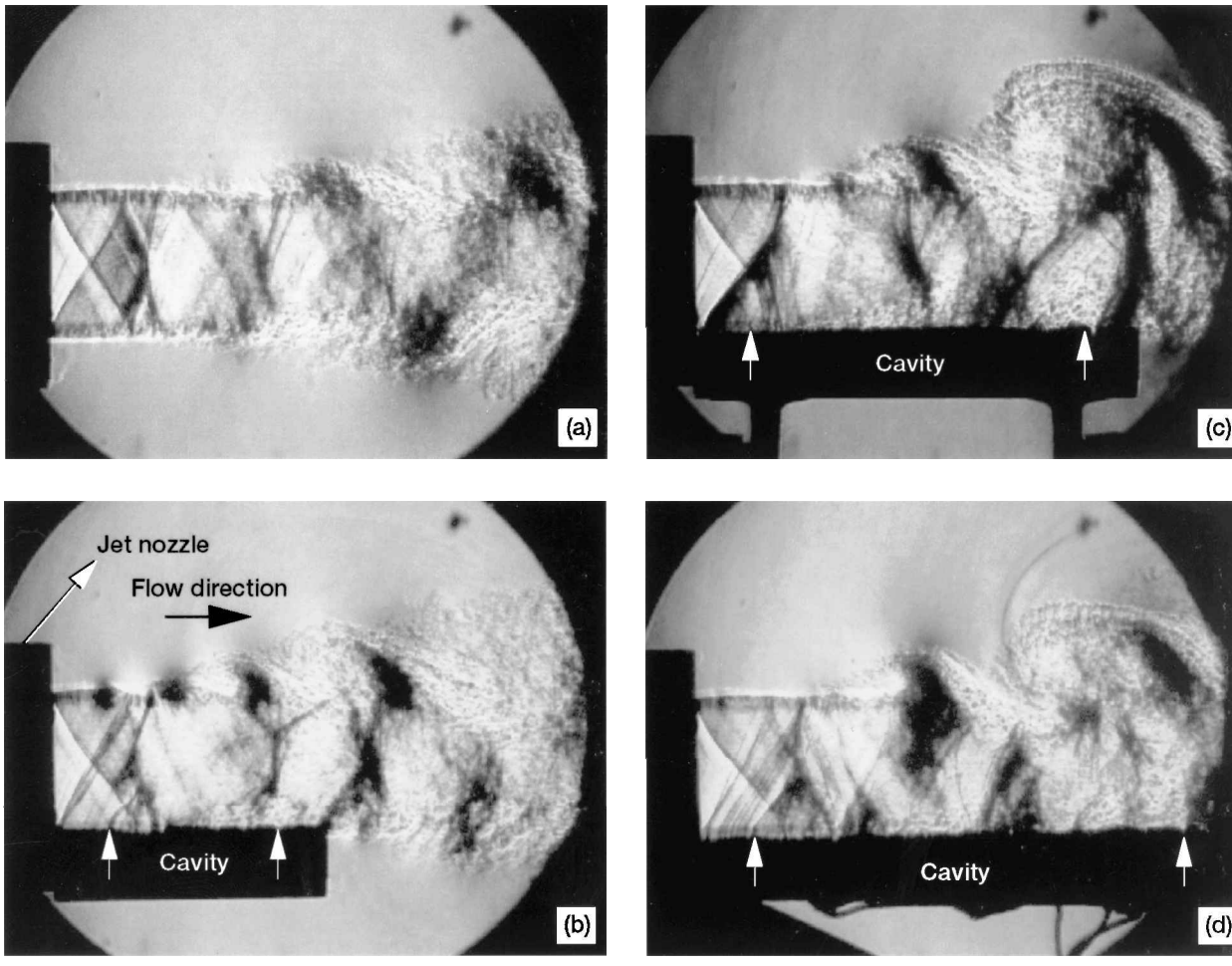

Fig. 3 Spark-schlieren photographs of jet–cavity interaction at $M_j = 1.1$, view shows narrow dimension of jet: a) jet without cavity and b–d) jet with cavity with different L/D: b) 3, c) 6, and d) 8. White arrows mark upstream and downstream edges of cavity.

to 2400 Hz at $M_j = 1.32$. A peak screech amplitude of 135 dB was recorded during the experiments. The frequency vs M_j for jet screech shown in Figs. 5a and 5b can be easily predicted using relationships proposed by Powell[1] and Tam.[34]

Although the screech modes appear to be independent of cavity tones, they may still influence mode IB for the $L/D = 3$ cavity and modes IIIB and IIB for the $L/D = 8$ cavity. For the most part, the cavity tone frequencies appear to increase with M_j, whereas the screech tone frequency decreases with M_j. This may initially come as a surprise because the mechanisms for tone production are remarkably similar. However, one should recognize that, in the screech problem, the shock-cell length increases with M_j and that its increase with M_j is more than twice the increase in convective velocity, thus, the decrease in frequency with increase in M_j. In contrast, for jet–cavity interaction, the location of the downstream edge is fixed, and the travel time for disturbances to reach the edge decreases with increasing M_j, leading to the increase in frequency with M_j.

The data of Fig. 6 show that the cavity tone's amplitude measured using a microphone within the cavity is both mode and Mach number dependent. Tone amplitudes generally increase with M_j, and multiple modes are present at mode transitions. The peak amplitudes are as high as 169 dB within the cavity. Furthermore, Fig. 6 also gives us a qualitative idea of the exchange of energy between the various modes. For example, in the $L/D = 3$ cavity (Fig. 6a) when the amplitude of mode III decays, modes IA and IIA are augmented. At higher Mach numbers, a drop in the amplitude of mode IIB is accompanied by the increase in that for IB. Similarly, for the $L/D = 8$ cavity (Fig. 6b), the appearance of mode IIIA is coincident with a change in the slope of the amplitude of mode IIA. Again, at higher Mach numbers, when mode I diminishes, mode IIIB is augmented, which, in turn, gives way to mode IIB.

C. Models for Tones Observed in the Experiments

Correlations for nondimensional tone frequencies (Helmholtz numbers[10]) produced by both cavities are shown in Fig. 7. Simple correlations for our experimental data are shown (solid lines). In addition, the Rossiter[6,7] equation (dashed line) is plotted for comparison. One unique feature of our jet–cavity configuration is that, theoretically, both screech and cavity tones are permissible. Which, if any, of these tones appear is quite easily checked. If screech tones were present, then one would expect them to at least qualitatively be predicted by Powell's[1] formula, given by

$$f = U_c/S(1 + M_c) \tag{1}$$

where f is the screech frequency, U_c is the convective speed of the hydrodynamic disturbance, S is the shock spacing, M_c is the convective Mach number (U_c/a), and a is the speed of sound in the ambient medium. On the other hand, if cavity tones dominate the spectrum, then they would be predicted by the modified Rossiter equation, which can be represented as

$$\frac{fL}{U_0} = \frac{(m - \zeta)}{\left[M_\infty \Big/ \sqrt{1 + (\gamma - 1)/2M_\infty^2} + 1/k_v\right]} \tag{2}$$

where

k_v = ratio of disturbance convection velocity to free stream velocity, U_c/U (value of 0.57 suggested by Rossiter)
L = cavity length
M = freestream Mach number
m = integers representing mode numbers, 1, 2, and 3
ζ = empirical constant, 0.25

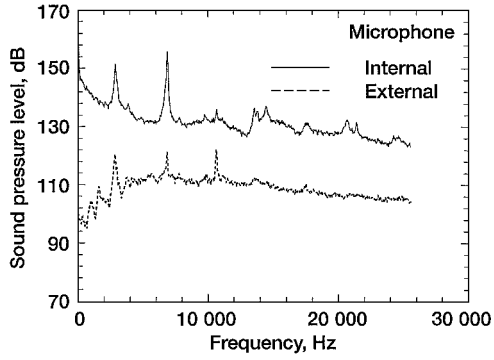

a) Spectra from external and internal (cavity) microphones

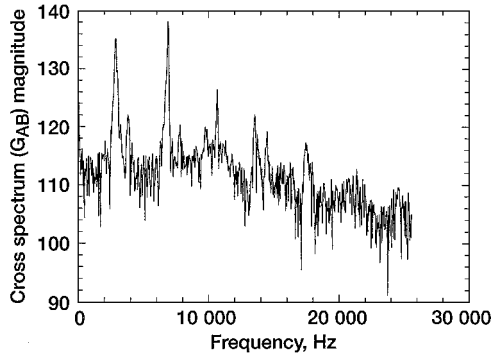

b) Cross-spectrum magnitude

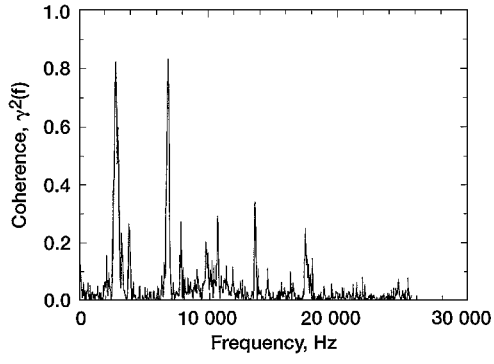

c) Linear spectral coherence

Fig. 4 Narrowband spectra from two-point microphone measurements, $M_j = 1.19$, $L/D = 3$ cavity. Internal microphone flush mounted on cavity floor at $x/D = 0.7$ and $y/D = 0$; external microphone at $r/D = 16$, oriented at 45 deg on the xy plane (see Fig. 1).

An explicit comparison with Powell's equation is not shown because our experiments showed that screech tones that were present in the jet without the cavity were absent when the cavity was added. Several researchers, including Heller et al.[14] and Tam and Block[13] have shown that the Rossiter equation can only correlate a small subset of all cavity tones. Although the Rossiter equation does not predict our data accurately, it does predict trends for the $L/D = 3$ cavity (Fig. 7a) but is completely incongruous with our $L/D = 6$ and 8 cavities (Figs. 7b and 7c). Therefore, it appears that jet–cavity interactions for the $L/D = 3$ case do have some resemblance to a cavity in an infinite flight stream. However, our experimental results do exhibit clear trends for which we seek correlations. The $L/D = 3$ cavity frequencies are well correlated by a Helmholtz number,[10] given by

$$fL/a_0 = 0.3nM_j^{\frac{1}{2}}, \qquad n = 1, 2, 3 \tag{3}$$

and the $L/D = 6$ and 8 results correlate with

$$fL/a_0 = (n + 1)/4, \qquad n = 1, 2, 3 \tag{4}$$

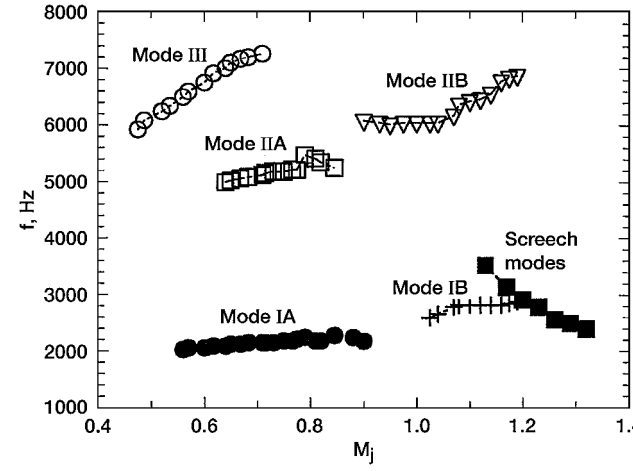

a) $L/D = 3$ cavity

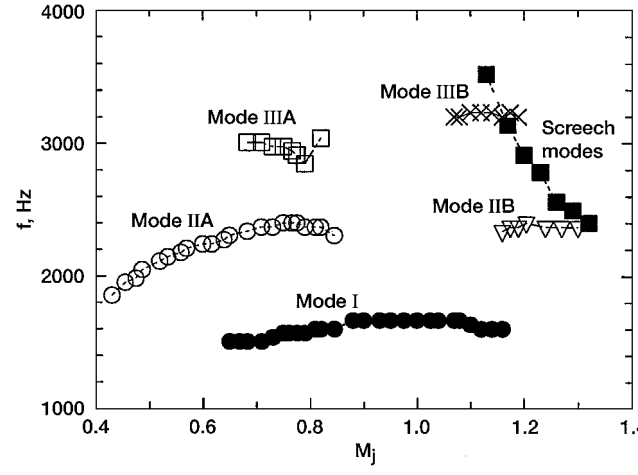

b) $L/D = 8$ cavity

Fig. 5 Frequency of tone produced by jet–cavity interaction vs fully expanded jet Mach number.

In both Eqs. (3) and (4), f represents the frequency of the tone; L the cavity length; a_0 and M_j the ambient sound speed and the fully expanded jet Mach number, respectively; and n the mode index.

A distinct result in Fig. 7 is that the Helmholtz number[10] is dependent on M_j for the $L/D = 3$ cavity, but independent of it for cavities having L/D of 6 and 8. We can, thus, classify jet–cavity interaction tones to be of two types. Type 1 (T1) when the Helmholtz number[10] depends on M_j and type 2 (T2) when the Helmholtz number is independent of M_j. Tones of type T1 are observed in the $L/D = 3$ cavity, whereas cavities with $L/D = 6$ and 8 produce tones of type T2. For T1, it is remarkable that although the flow stream changes from subsonic to supersonic (shock containing) a simple relationship [Eq. (3)] is still able to correlate the frequency data over the entire Mach number range.

Equation (4) for the $L/D = 8$ cavity can easily be reconciled with Tam's[12] calculated normal mode frequencies for rectangular cavities as follows. Tam and Block[13] calculated the acoustic modes of rectangular cavities with no flow and showed that considerable insight can be obtained by examining these solutions. If we consider Tam's[12] calculated frequency (the real part of $\omega L/a$, where $\omega = 2\pi f$ and a is the speed of sound in the ambient medium) plotted vs D/L for the lowest normal mode (cavity mode 1, 1), then the frequency corresponding to $L/D = 8$ is $\omega L/a = 3$. On rewriting this, it becomes $fL/a_0 = 0.48$, which corresponds to the lowest mode of our correlation. It is indeed surprising that, despite the complexity of the source region and the flow within the cavity, the frequencies are predicted using the acoustic modes of the cavity (calculated without flow).

Before concluding this section, it is important to comment on the state of the initial boundary layer upstream of the cavity. Our

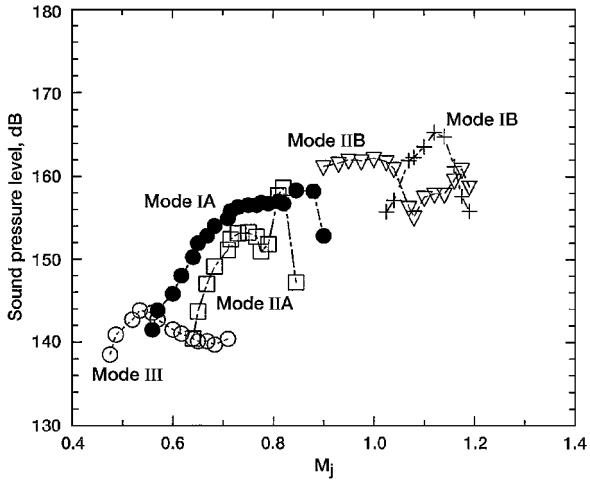

a) *L/D* = 3 cavity

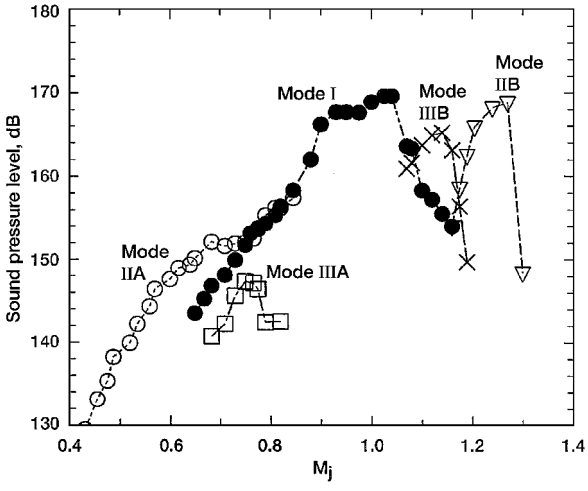

b) *L/D* = 8 cavity

Fig. 6 Tone amplitude produced by jet–cavity interaction vs fully expanded jet Mach number.

nozzle/transition piece was 18.96 cm long, and a critical Reynolds number of approximately 3×10^5 was attained at a very low jet Mach number of 0.07. Because our experiments were conducted over a range of Mach numbers from 0.4 to 1.3, the nozzle exit boundary layer can be justifiably assumed to be turbulent for all cases. Estimated values of boundary-layer thickness just upstream of the cavity obtained using $\delta/x = 0.16/Re_L^{1/7}$ were 3.8 mm at $M_j = 0.4$ and 3.22 mm at $M_j = 1.3$, yielding an average value of 3.51 mm over the entire Mach number range. Furthermore, note that the values of δ/L were 0.092, 0.046, and 0.034 for cavities having L/D ratios of 3, 6, and 8, respectively. Interestingly, Rossiter's.[6,7] value was 0.081, which is close to the value for our $L/D = 3$ cavity, for which the primary mode is reasonably well predicted by Rossiter's equation.

D. Pressure Variations on the Cavity Floor

In a recent paper, Stallings and Wilcox[22] reviewed the various classifications of cavity flows. In addition to classifying cavities as being deep (small L/D) or shallow (large L/D), we can also classify cavity flows as being open, closed, or transitional. When the shear layer spans the cavity opening, the cavity is considered open, and when the shear layer attaches to the cavity floor, the cavity is considered closed. Intermediate stages are transitional. Though much is known about the types of cavity flows, researchers still cannot agree on exact definitions. For example, Rossiter[7] defined deep cavities as having $L/D < 4$ and shallow cavities having $L/D > 4$. In contrast, Heller et al.[15] and Shaw and McGrath[24] defined $L/D = 1$ as the dividing line to define deep and shallow cavities. The same is true of open, transitional, and closed cavity flows. Stallings and

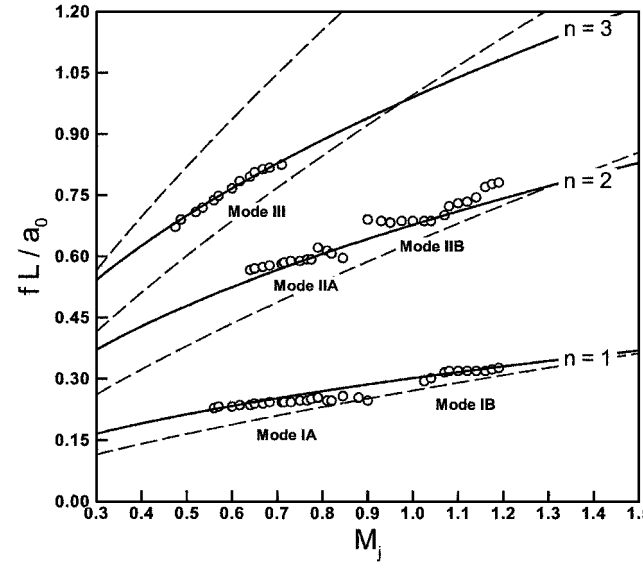

a) *L/D* = 3 cavity

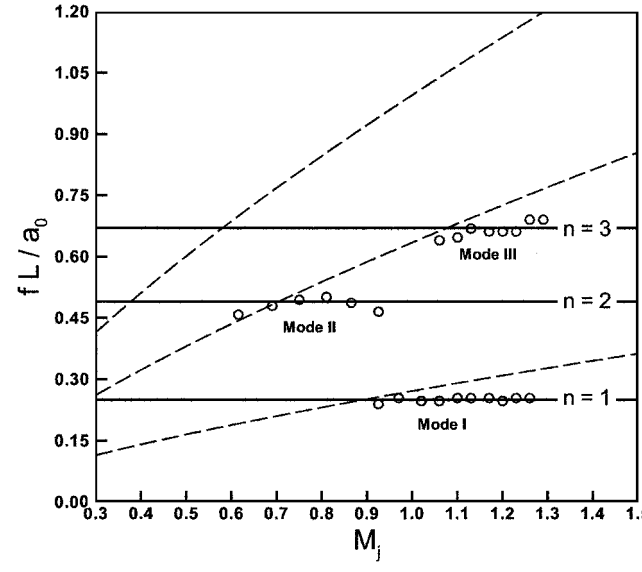

b) *L/D* = 6 cavity

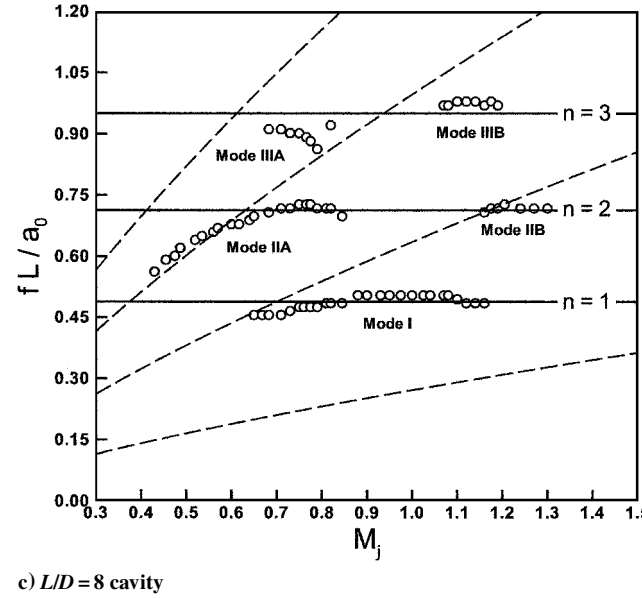

c) *L/D* = 8 cavity

Fig. 7 Correlation for normalized frequency vs fully expanded jet Mach number: – – –, modified Rossiter equation and ——, correlation proposed in the present paper.

Wilcox,[22] Plentovich et al.,[23] and Shaw and McGrath[24] use very wide and differing bands to define these cavity types. Such startling discrepancies provided us with the impetus for conducting a detailed study of the pressure distribution on the floor of the cavity for cavities with $L/D = 3$ and 8 over a range of Mach numbers. We chose the PSP technique because of the high spatial resolution it provides (equivalent to about 250,000 pressure taps) and because of our extensive previous experience with this technique in studying ejector wall pressures.[35]

When comparing the pressure distributions used by Stallings and Wilcox[22] to define open, transitional, and closed cavity flows with results of the present work, we should note two points. First, Stallings and Wilcox[22] defined C_p as $(p - p_\infty)/q_\infty$, where p is the cavity floor pressure, p_∞ the freestream static pressure, and q_∞ the freestream dynamic pressure. Our definition differs because we use $C_p = (p - p_a)/p_a$, where p is the cavity floor pressure and p_a is the ambient pressure. Second, the Stallings and Wilcox[22] diagrams are valid only for a supersonic flight stream. In comparison, our flow comprises subsonic, sonic, and supersonic shock-containing jets interacting with a cavity. However, we can still make useful qualitative comparisons with the Stallings and Wilcox[22] classifications.

Results for the $L/D = 8$ cavity shown in Figs. 8 and 9 are interesting because all three types (open, closed, and transitional) of cavity flows were possible here. In addition, we note a very intriguing trend as the Mach number increases. Careful scrutiny of the pressure maps reveals that the presence of 1) a subatmospheric pressure region immediately after the upstream edge of the cavity and 2) a high-pressure region closer to the downstream edge of the cavity. Note the spanwise variation in the pressure near the downstream edge of the cavity. (Color copies of Fig. 8 are available from the authors.) As the Mach number increases from 0.615 to 0.97, the pressure values and axial extent of the low-pressure region decrease, whereas the pressures and the extent of the downstream high-pressure region increase. However, at supersonic Mach numbers ($M_j = 1.02$–1.32) the trend reverses itself. Note not only the reversal of trend but also that $M_j = 1$ demarcates the reversal in trend. Based on the $C_p[C_p = (p - p_a)/p_a]$ profiles in Fig. 9, it appears that for $M_j = 0.615$–0.865, the cavity is transitional. At $M_j = 0.97$ and 1.02, it becomes closed, and finally, it becomes open at higher Mach numbers. Thus, our results emphasize the point that the open/closed classification of cavities distinctly depends on the Mach number. Thus, a cavity that is transitional at $M_j = 0.865$ could become closed at $M_j = 0.97$ and then suddenly become open at $M_j = 1.13$. These scenarios suggest that the lack of clear definitions perhaps arise due to the sensitivity of the shear layer to initial conditions, Mach number, and the presence and location of shocks.

We now provide a connection between the two parts of our paper. Based on the vivid display (Figs. 8 and 9) of several distinct flow regimes over a small M_j range for the $L/D = 8$ cavity, one would expect that it would be very difficult to predict the frequencies of tones produced by this cavity. Contrary to our expectations, a simple relationship from Sec. III.B [Eq. (4)] that depends only on the cavity's acoustic modes (and not on flow within the cavity) successfully correlates all tones.

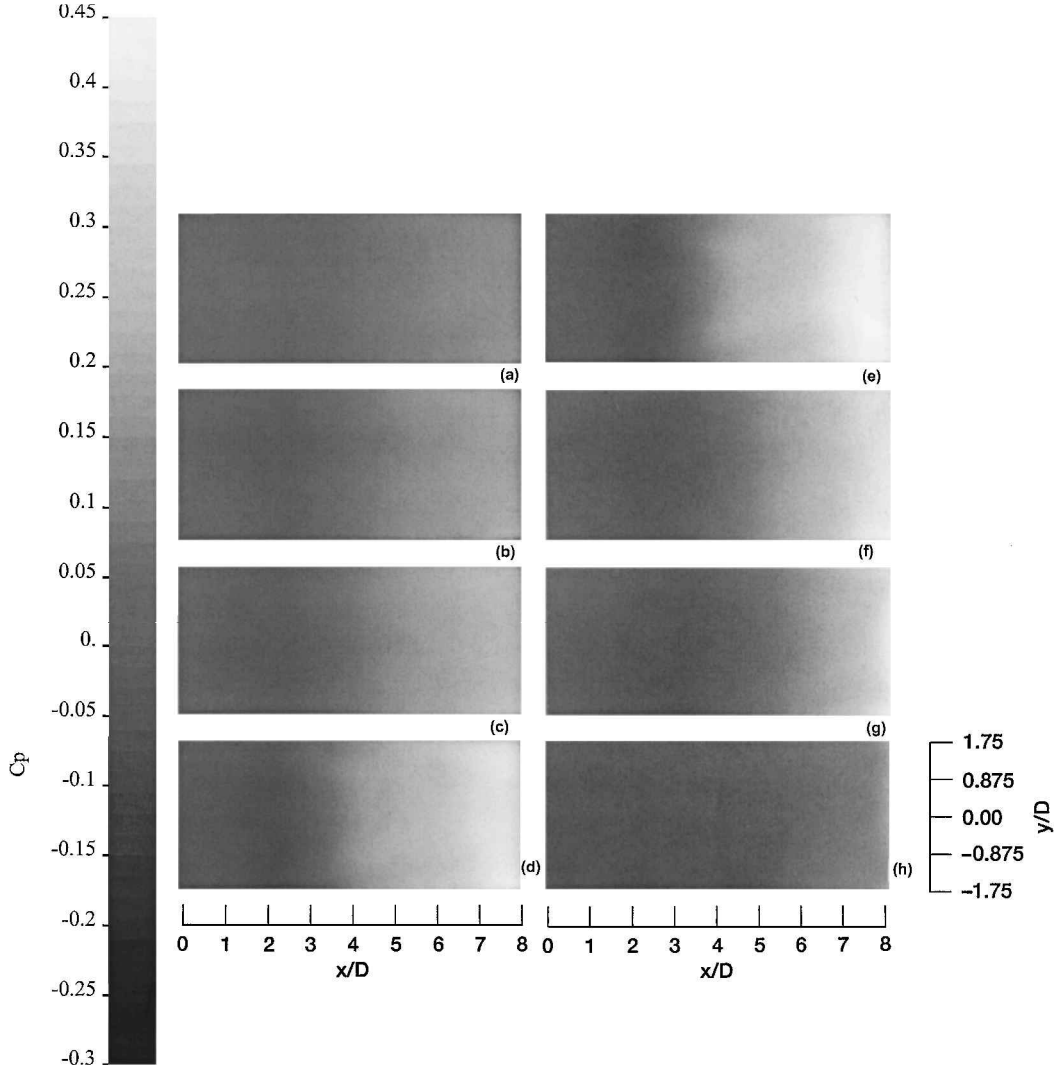

Fig. 8 Photoluminescent PSP results for the $L/D = 8$ cavity at various jet Mach numbers M_j: a) 0.615, b) 0.75, c) 0.865, d) 0.97, e) 1.02, f) 1.13, g) 1.23, and h) 1.32.

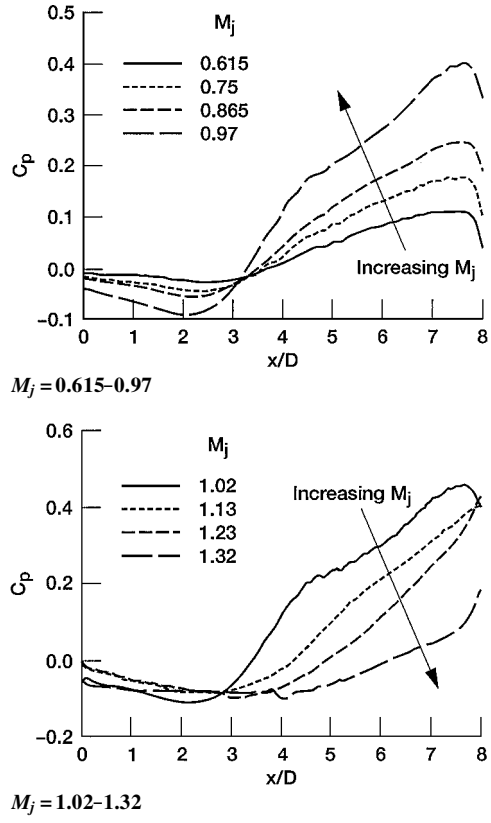

Fig. 9 Centerline pressure coefficients derived from PSP for the *L/D* = 8 cavity.

IV. Conclusions

Our study of jet–cavity interaction was motivated by the need to understand cavity flows well enough to devise effective cavity resonance suppression techniques. A series of experiments was performed on subsonic, sonic, and supersonic jets interacting with cavities having L/D ratios of 3, 6, and 8. In addition to spark-schlieren flow visualization and documentation of the tone frequencies and amplitudes of jets interacting with cavities, we also provided spectra of near-field unsteady pressures. Time-averaged pressures on the cavity floor were studied using the novel photoluminescent PSP technique that had high spatial resolution and revealed complex pressure distributions on the cavity floor. Our study resulted in two important findings:

1) In addition to previous classifications of cavity tones, the Helmholtz number[10] H can be used to classify all jet–cavity tones into two types. In T1, H is dependent on the flow Mach number, and in T2, it is independent. We propose simple correlations for both types of tones. Whereas the former type of tones appear to be produced by shear layer instabilities enhanced by acoustic feedback, the latter type of tones are determined solely by the cavity's natural acoustic modes. T1 tones appeared in cavities with an length/depth (L/D) ratio of 3, whereas T2 tones that were previously believed to be present only at low Mach numbers dominated in cavities with $L/D = 6$ and 8 at both high subsonic and supersonic Mach numbers. Although we have reason to believe that we now have a better understanding of jet–cavity flows, we reiterate that, to date, no theory can predict the amplitude of cavity tones. Furthermore, notwithstanding our proposed relationships that can correlate the two types of jet–cavity tones, a clear explanation for why and when modes I–III appear is still not forthcoming.

2) Previous research led us to expect that traditional classifications (open, transitional, or closed) for cavities in an infinite flight stream would be insensitive to small changes in Mach number and would depend primarily on cavity L/D ratios. Use of the novel high-resolution photoluminescent PSP shows that the classifications are actually quite sensitive to jet Mach number for an $L/D = 8$ cavity. However, these classifications provide no guidance whatsoever for tone types, amplitude, or frequency. Additionally, although the pressure patterns on the cavity floor display very complex variations with the Mach number for an $L/D = 8$ cavity, T2 tones that are independent of flow Mach number dominate. For an $L/D = 3$ cavity, however, a surprise emerges: The pressure patterns on the cavity floor are not so complex, but the tones are T1 and depend significantly on the flow. It is hoped that the detailed experimental data and insights presented here will be useful to those devising cavity resonance suppression techniques for use in practical applications and to those performing numerical simulations of jet–cavity flows.

References

[1]Powell, A., "On the Mechanism of Choked Jet Noise," *Proceedings of the Physical Society, London*, Vol. 66, 1953, pp. 1039–1056.

[2]Powell, A., "On the Edgetone," *Journal of the Acoustical Society of America*, Vol. 33, 1961, pp. 395–409.

[3]Crighton, D. G., "The Jet Edge-Tone Feedback Cycle; Linear Theory for the Operating Stages," *Journal of Fluid Mechanics*, Vol. 234, 1992, pp. 361–392.

[4]Howe, M. S., "Edge, Cavity and Aperture Tones at Very Low Mach Numbers," *Journal of Fluid Mechanics*, Vol. 330, 1997, pp. 61–84.

[5]Raman, G., "Advances in Understanding Supersonic Jet Screech: Review and Perspective," *Progress in Aerospace Sciences*, Vol. 34, 1998, pp. 45–106.

[6]Rossiter, J. E., "The Effect of Cavities on the Buffeting of Aircraft," Royal Aircraft Establishment, TM 754, 1962.

[7]Rossiter, J. E., "Wind-Tunnel Experiments on the Flow Over Rectangular Cavities at Subsonic and Transonic Speeds," Aeronautical Research Council, Repts. and Memorandum 3438, 1966.

[8]East, L. F., "Aerodynamically Induced Resonance in Rectangular Cavities," *Journal of Sound and Vibration*, Vol. 3, 1966, pp. 277–287.

[9]Bilanin, A. J., and Covert, E. E., "Estimation of Possible Excitation Frequencies for Shallow Rectangular Cavities," *AIAA Journal*, Vol. 11, No. 3, 1973, pp. 347–351.

[10]Helmholtz, H. L. F., *Sensations of Tone*, 2nd ed., Dover, New York, 1954.

[11]Block, P. J. W., "Noise Response of Cavities of Varying Dimensions at Subsonic Speeds," NASA TN D-8351, 1976.

[12]Tam, C. K. W., "The Acoustic Modes of a Two-Dimensional Rectangular Cavity," *Journal of Sound and Vibration*, Vol. 49, 1976, pp. 353–364.

[13]Tam, C. K. W., and Block, P. J. W., "On the Tones and Pressure Oscillations Induced by Flow Over Rectangular Cavities," *Journal of Fluid Mechanics*, Vol. 89, 1978, pp. 373–399.

[14]Heller, H. H., Holmes, D. G., and Covert, E. E., "Flow-Induced Pressure Oscillations in Shallow Cavities," *Journal of Sound and Vibration*, Vol. 18, 1971, pp. 545–553.

[15]Heller, H., Widnall, S., Jones, J., and Bliss, D., "Water Table Visualization of Flow Induced Pressure Oscillations in Shallow Cavities for Simulated Supersonic Flow Conditions," Acoustical Society of America, Paper Z13, 1973.

[16]Heller, H. H., and Bliss, D. B., "Physical Mechanism of Flow-Induced Pressure Fluctuations in Cavities and Concepts for Their Suppression," AIAA Paper 75-491, 1975.

[17]Rockwell, D., and Naudascher, E., "Review of Self-Sustaining Oscillations of Flow Past Cavities," *Journal of Fluids Engineering*, Vol. 100, 1978, pp. 152–165.

[18]Komerath, N. M., Ahuja, K. K., and Chambers, F. W., "Prediction and Measurement of Flows Over Cavities a Survey," AIAA Paper 87-022, 1987.

[19]Chokani, N., "Flow-Induced Oscillations in Cavities: A Critical Survey," DGLR/AIAA Paper 92-02-159, 1992.

[20]Shaw, L. L., "Suppression of Aerodynamically Induced Cavity Oscillations," U.S. Air Force Flight Dynamics Lab., AFFDL-TR-79-3119, 1979.

[21]Lucas, M. J., Noreen, R. A., Sutherland, L. C., Cole, J. E., III, and Junger, M. C., *Handbook of the Acoustic Characteristics of Turbomachinery Cavities*, American Society of Mechanical Engineers, New York, 1997.

[22]Stallings, R. L., Jr., and Wilcox, F. J., Jr., "Experimental Cavity Pressure Distributions at Supersonic Speeds," NASA TP-2683, 1987.

[23]Plentovich, E. B., Stallings, Jr., R. L., and Tracy, M. B., "Experimental Cavity Pressure Measurements at Subsonic and Transonic Speeds," NASA TP 3358, 1993.

[24]Shaw, L. L., and McGrath, S., "Weapons Bay Acoustics: Passive or Active Control," AIAA Paper 96-1617, 1996.

[25]Cattafesta, L. N., III, Garg, S., Choudhari, M., and Li, F., "Active Control of Flow-Induced Cavity Resonance," AIAA Paper 97-1804, 1997.

[26]Kavandi, J., Callis, J., Gouterman, M., Khalil, G., Wright, D., Green, E., Burns, D., and McLachlan, B., "Luminescent Barometry in Wind Tunnels," *Review of Scientific Instruments*, Vol. 6, 1990, pp. 3340–3347.

[27]McLachlan, B. G., Kavandi, J. B., Callis, J., Gouterman, M., Khalil, G., and Burns, D., "Surface Pressure Field Mapping Using Luminescent Coatings," *Experiments in Fluids*, Vol. 14, 1993, pp. 33–41.

[28]Morris, M. J., and Donovan, J. F., "Application of Pressure and Temperature Sensitive Paint to High-Speed Flows," AIAA Paper 94-2231, 1994.

[29]Bencic, T. J., "Experiences Using Pressure Sensitive Paint in NASA Glenn Research Center Propulsion Test Facilities," AIAA Paper 95-2831, 1995.

[30]Bencic, T. J., "Rotating Pressure and Temperature Measurement on Scale Model Fans Using Luminescent Paints," AIAA Paper 98-3452, 1998.

[31]Oglesby, D. M., Upchurch, B. T., Leighty, B. D., Simmons, K. A., and Demandante, C. G., "Pressure Sensitive Paint with Internal Temperature Sensing Luminophore," *Proceedings of the 42nd Instrument Symposium of the ISA*, Instrumentation Systems and Automation Society, Research Triangle Park, NC, 1996, pp. 205–224.

[32]Umeda, Y., and Ishii, R., "Reduction of Noise Radiated from Supersonic Jet by Interaction Between the Screech and Cavity Tones," American Society of Mechanical Engineers, Paper FEDSM 98-5240, 1998.

[33]Gharib, M., and Roshko, A., "The Effect of Flow Oscillations on Cavity Drag," *Journal of Fluid Mechanics*, Vol. 177, 1987, pp. 501–530.

[34]Tam, C. K. W., "The Shock Cell Structures and Screech Tone Frequencies of Rectangular and Nonaxisymmetric Supersonic Jets," *Journal of Sound and Vibration*, Vol. 121, 1988, pp. 135–147.

[35]Taghavi, R., Raman, G., and Bencic, T., "Visualization of Ejector Wall Pressure Using Pressure Sensitive Paint," American Society of Mechanical Engineers, Paper FEDSM 97-3236, 1997.

P. J. Morris
Associate Editor